Article

Modification of the Leeb Impact Device for Measuring Hardness by the Dynamic Instrumented Indentation Method

Aleksander Umanskii *, Kirill Gogolinskii [ID]**, Vladimir Syasko and Artem Golev**

Department of Metrology, Instrumentation and Quality Management, Saint-Petersburg Mining University, 199106 Saint-Petersburg, Russia; gogolinskiy_kv@pers.spmi.ru (K.G.); 9334343@gmail.com (V.S.); artemgolev1999@gmail.com (A.G.)
* Correspondence: umanskiy_as@pers.spmi.ru

Abstract: The article is devoted to modification of the impact devices of Leeb hardness testers for the implementation of the dynamic instrumented indentation method. The results obtained made it possible to construct a load–displacement curve using primary EMF signals and made it possible to determine the values of the dissipated and elastic impact body energy, the maximal load of indentation, the maximal and residual penetration depth and the geometric parameters of the indentation region, namely the contact area of the indenter with the surface and the volume of the displaced material. The listed parameters of the indentation process allow us to measure the contact and volume hardness, the elastic modulus and the yield strength of test objects with portable hardness testers.

Keywords: hardness; portable hardness tester; rebound hardness test; dynamic instrumented indentation

1. Introduction

Hardness is a widely used measurement for determining the various elastic, plastic and brittle properties of solid bodies. [1]. There are many different methods for measuring hardness, differing in the shape of the indenter, the method of applying the load, the algorithm for calculating hardness, etc. [2]. Various methods of hardness measurement can be divided according to the rate of application of the load into static (quasi-static) and dynamic types. For example, Brinell, Rockwell and Vickers hardness are referred to as static, but Shore and Leeb hardness are referred to as dynamic [3]. Devices that implement static methods are mainly used in laboratories; to carry out measurements with them, it is often necessary to cut out samples. Various types of portable hardness testers are used to measure mechanical properties directly on test objects [4]. The data obtained using most common portable hardness testers [5] are indirectly related to standardized hardness scales according to empirical formulas or experimental conversion tables obtained for a specific type of material [6]. In addition, they have a number of restrictions in terms of the thickness and weight of the test sample. Despite these features, portable hardness testers are widely used for the inspection of welding joints in pipelines, building structures, etc. [7,8]. Currently, some of the most common types of portable hardness testers are dynamic Leeb hardness testers [9,10].

Dynamic indentation methods are widely used for measuring the elastic–plastic properties of materials, such as the elasticity modulus, yield strength and strain hardening coefficient. They are used to study the properties of a wide range of materials from elastomers [11] to superhard crystals [12]. The theoretical foundations of dynamic hardness were described in [13] and generalized in [14]. Investigations of the specifics of plastic deformation and strain hardening during dynamic indentation have been presented in other works [15–17]. Much attention has been paid to numerical modeling of the processes of interaction between the indenter and the sample during dynamic indentation [18–21].

Research into and development of devices and methods of dynamic indentation were carried out by the authors of other works [22–24].

For experiments applying dynamic indentation, it is necessary to standardize the mass and velocity of the impactor's body, as well as the material and shape of the indenter (radius of the spherical indenter). During the calculation of the experimental data, the time of various phases of the impact, the energy dissipated during the impact, the penetration depth, etc. can be analyzed. Full information about the impact can be obtained by measuring the time dependence of the force applied during the interaction of the impact body with the surface, and the penetration depth. The resulting plot of applied force and penetration depth $P(h)$ is similar to the representation of data in the instrumented indentation method [25], so this method can be called dynamic instrumented indentation (DII). However, in contrast to quasi-static instrumented indentation, there is currently no generally accepted unified theory for the analysis of dynamic $P(h)$ curves. The greatest success in the development of methods and tools for dynamic instrumented indentation was achieved by Rudnitskiy and colleagues [26,27]. Using a portable impact hardness tester of their own design, they demonstrated the possibility of measuring the elastic modulus [28], the yield strength [29] and the strain hardening coefficient of metals [30]. The disadvantage of these results was the gravitational method of impact body acceleration used in the impact device, which allowed them to perform measurements only on a horizontal surface, as well as the lack of uniform requirements for the impact devices and, as a consequence, the impossibility of obtaining comparable data. The solution to this problem is the use of Leeb hardness testers [31]. The disadvantage of the existing Leeb hardness testers is that they actually measure the coefficient of restitution: the ratio of the rebound velocity of the impact body to the impact velocity, which, according to [14], is a function of the elasticity modulus to the dynamic yield strength ratio E/Y_d. To implement the DII method with Leeb hardness testers, it is necessary to modify the impact device, as well as the data collection and processing methods. The results thus obtained make it possible to construct a load–displacement curve using the primary EMF signal and to obtain the values of the impact body's energy for determining the penetration depth and the geometric parameters of the indentation region, namely the contact area of the indenter with the surface and the volume of the displaced material. The listed parameters of the indentation process allow use to measure the contact and volume hardness, elastic modulus and yield strength of test objects with portable hardness testers.

2. Materials and Methods

The Leeb method is based on measuring the velocity of the impact body (Figure 1) v_A during the fall and the rebound v_R after the impact on the test piece. At the same time, the values of the maximum (impact velocity v_A) and minimum (rebound velocity v_R) velocity are fixed. Flying through the induction coil, the magnet located inside the impact body induces an EMF in it, proportional to the rate of impact velocity (Figure 2). After hitting the surface of the test object, the impact body bounces off and the magnet located inside it induces an EMF in the induction that is proportional to the rebound velocity (2). Leeb hardness HL is calculated on the basis of the ratio [9]:

$$HL = 1000 \frac{v_R}{v_A}, \tag{1}$$

where v_R is the rebound velocity and v_A is the impact velocity. In accordance with the current standard, the induction coil is located in such a way that the EMF peak occurs at a certain distance between the impact body and the surface of a test piece (no more than 2 mm).
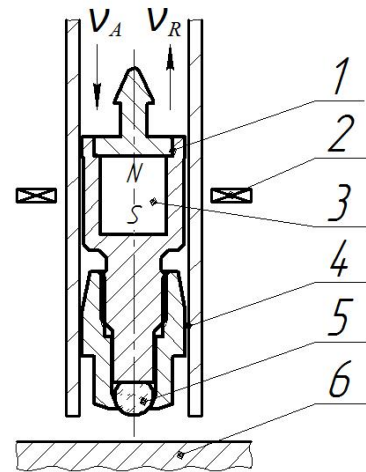
Figure 1. Leeb hardness measuring scheme: 1—impact body, 2—induction coil, 3—magnet, 4—guiding tube; 5—indenter; 6—test piece.
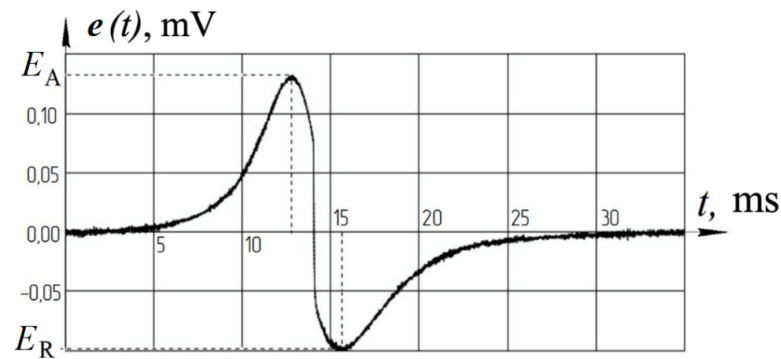
Figure 2. Graph of EMF *e*(*t*), induced in induction coil during measurement.

The specificity of the measuring process imposes certain restrictions on the scope of this method. In the Leeb test, the measurement result can be influenced by the thickness and mass of the part.

The essence of the method of DII is to receive the EMF signal of the impact device, convert it into a velocity signal and calculate it in order to obtain the dependences of the applied force and the resulting deformation in the indentation process. In this case, the calibration of the impact device and obtaining the factor for conversion of the EMF into the velocity has been carried out by various methods [32,33].

To plot the load–displacement curve, the velocity signal can be described as:

$$V(t) = k \cdot e(t) \tag{2}$$

where V is the impact velocity, in $\frac{m}{s}$; k is the EMF conversion factor and $e(t)$ is the signal, obtained during testing (EMF).

Calculation of the penetration depth in time $h(t)$ was according to the expression:

$$h(t) = \int_{t_0}^{t} V(t)dt \tag{3}$$

The calculation of the contact load in time $P(t)$ occurs according to the expression:

$$P(t) = m\alpha(t) = m\frac{dV(t)}{dt} \tag{4}$$

where m is the mass of the impact body and a is the acceleration.

Given the values of penetration depth and force, a load–displacement curve can be plotted $P(h)$.

The processing of the raw EMF signal and its conversion to the velocity signal, as well as further numerical integration and differentiation, made it possible to obtain the values of the impact body energy to determine the penetration depth and the geometric parameters of the indentation region, namely the contact area of the indenter with the surface and the volume of the displaced material. With the listed data, it was possible to calculate [2] the contact hardness, the yield stress, and the elasticity modulus.

The primary EMF signal of the Leeb impact device is nonlinear in the area of the indentation process. The nonlinearity of the signal can lead to a significant error in the measurement results when constructing the load–displacement curve. For the correct calculation of the penetration depth, it was necessary to shift the penetration stage into the linear region of the impact device's transfer curve.

3. Results

To solve this problem, it was necessary to modify the design of the impact devices of Leeb hardness testers. This article considered a Type D Leeb impact device, as is this type of device that is most widespread in the market.

The impact device meets the requirements for its metrological characteristics, which are regulated by ISO standards [31].

The transfer curve of the impact device based on the induction coil is nonlinear in most of the range of distances between the impact body (magnet) and the coil. To solve the problem of plotting the impactor velocity signal, it is necessary to measure the EMF induced in the coil at the point of contact between the indenter and the surface of the test piece, i.e., at a time interval of no more than 100 µs when the indenter travels no more than 100 µm. Thus, it was necessary to ensure that the measurements of the EMF in the linear area of the impact device's transfer curve, which corresponds to the upper section of the curve, were taken when the impact body moves right through.

To achieve the required result, a mathematical model was used for the optimal placement of the induction coil relative to the permanent magnet [34]. At the moment of contact of the indenter tip with the surface of the test piece, the optimal distance from the permanent magnet to the induction coil (in mm) can be determined by the formula:

$$l = 0.72\frac{d_k}{d_m} - 1.75 \tag{5}$$

where d_m is the magnet's diameter, in mm, and d_k is the internal diameter of the induction coil, in mm. The required geometric arrangement of the impact device parts is shown in Figure 3.
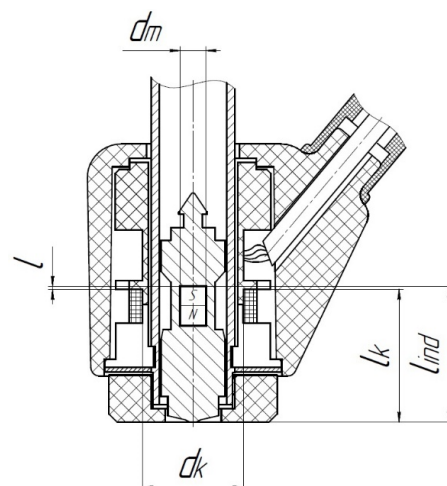
Figure 3. The location of the impact body relative to the induction coil at the time of indentation.

The parameters of the Type D impact device used in this study were d_k = 12 mm and d_m = 3 mm; by substituting these values into Equation (5), we obtained l = 1.13 mm.

The optimal distance (in mm) between the induction coil and the surface of the test piece was calculated by the formula:

$$l_k = l_{ind} - l \tag{6}$$

where l_{ind} is the impact body length from the end of the impact body (indenter) to the far edge of the magnet, which was equal to 16.5 mm. Substituting the obtained values of l and l_{ind} into Formula (6), we obtain:

$$l_k = 16.5 - 1.13 = 15.37 \; mm$$

Thus, for optimal results, the distance between the test surface and the edge of the coil was l_k = 15.37 mm.

The modification of the Leeb impact device for implementation of the DII method consisted of changing the position of the induction coil relative to the magnet. In the Type D transducers used in this study, this distance is l_D = 15.87 mm; therefore, the position of the inductor should be changed as follows:

$$\Delta l = l_D - l_k \tag{7}$$

Therefore, to perform the modification, the induction coil should be lowered by Δl = 0.5 mm (Figure 4). It can be achieved by lowering the induction coil itself or by decreasing the height of the support ring of the impact device. In addition, to implement the DII method, it was necessary to record EMF values with a sampling frequency of at least 2.5 MHz.

(a)   (b)
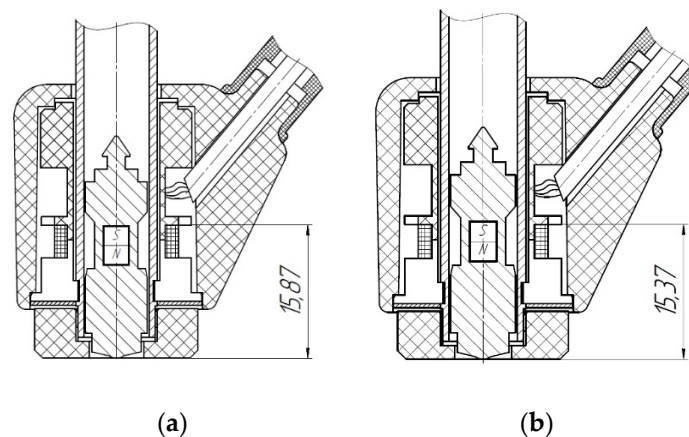
Figure 4. The position of the induction coil relative to the surface of test piece for standard (**a**) and modified (**b**) type D impact device.

To confirm the performance of the modifications made, a series of experiments was performed.

In the first experiment, two curves were reconstructed, one with the impact body flying through and one with the process of indentation into the surface of the test piece (Figure 5). When the signals are superimposed, it can be seen that the process of indentation into the material has shifted to the linear region of the impact device's transfer curve.
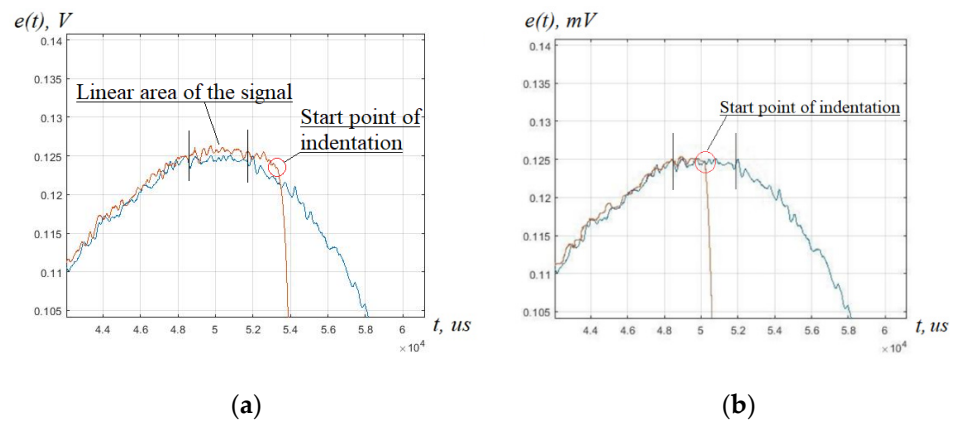
Figure 5. Signal obtained using a standardized (**a**) and modified (**b**) Leeb D impact device.

To confirm the efficiency of the technique, an experiment was carried out on aluminum test blocks, for which five measurements were made using a modified impact device. A computational method for load–displacement diagrams was applied to estimate the depth of the indentation; for comparison, each indentation was later checked using optical microscopy.

To construct the indentation diagrams, the EMF values were digitized at a frequency of 2.56 MHz by a 12-bit ADC. To filter the raw signal (Figure 6a), a low-pass filter with a bandwidth of 190 kHz was used. The velocity signal is shown in Figure 6b. Numerical integration and differentiation were carried out in MATLAB.
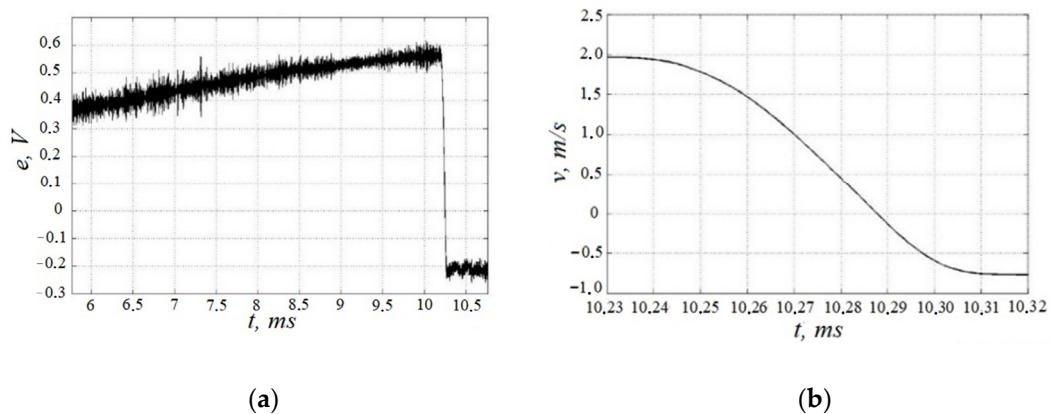

Figure 6. Graph of EMF *e*(*t*) induced on the induction coil during measurement (**a**) and graph of the impact body velocity during the indentation process (**b**).

Applying Formulas (3) and (4) described earlier, we obtained the graphs of the penetration depth versus time (Figure 7a) and the graph of the applied load versus time (Figure 7b).
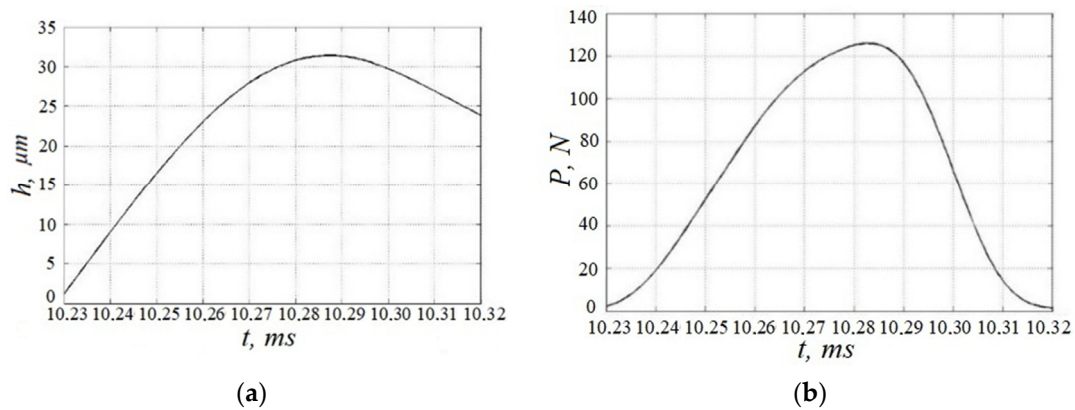
Figure 7. Graphs of the depth of penetration across time (**a**) and the graph of the applied load across time (**b**).

After construction of the dependence of the penetration depth on the load applied in the indentation process (Figure 8a), it was possible to calculate the residual indentation depth h_i. By measuring the indentation radius (Figure 8b) and knowing the function of the shape of the indenter, one can also calculate the residual indentation depth.
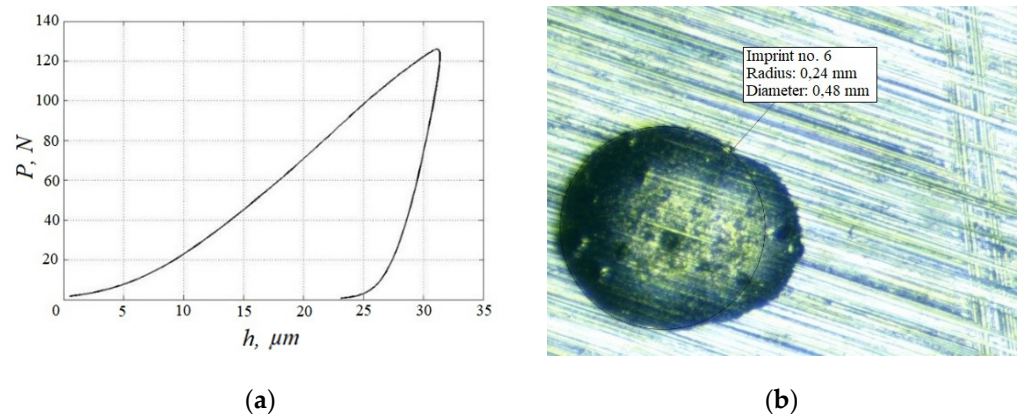
Figure 8. Load–displacement diagram (**a**) and photograph of the indentation (**b**).

The values of h_i obtained from five measurements on an aluminum test block by DII and an analysis of the load–displacement curve, and those obtained using a microscope are shown in Table 1.

Table 1. Measurement results.

№	Microscope, µm	DII, µm
1	22.0	22.8
2	22.7	21.2
3	19.6	19.9
4	19.2	19.0
5	20.3	21.4
Average	20.9	20.5
S. Deviation	1.9	1.6

As can be seen from the results of the experiment, if we take the measurements obtained by the microscope as the real values, the absolute error of the residual depth does not exceed 1.5 µm.

To confirm the applicability of the proposed technique on various types of materials, an experiment was carried out using the modified Leeb D impact device on three materials: aluminum, brass and steel, with a Vickers hardness of 30, 78 and 206 HV, respectively. The Vickers hardness values were obtained from direct measurements.

The obtained load–displacement curves corresponded to the typical nature of the curves obtained for these materials by the method of instrumented indentation, which confirms the possibility of using the proposed technique on a wide range of tested materials (Figure 9).
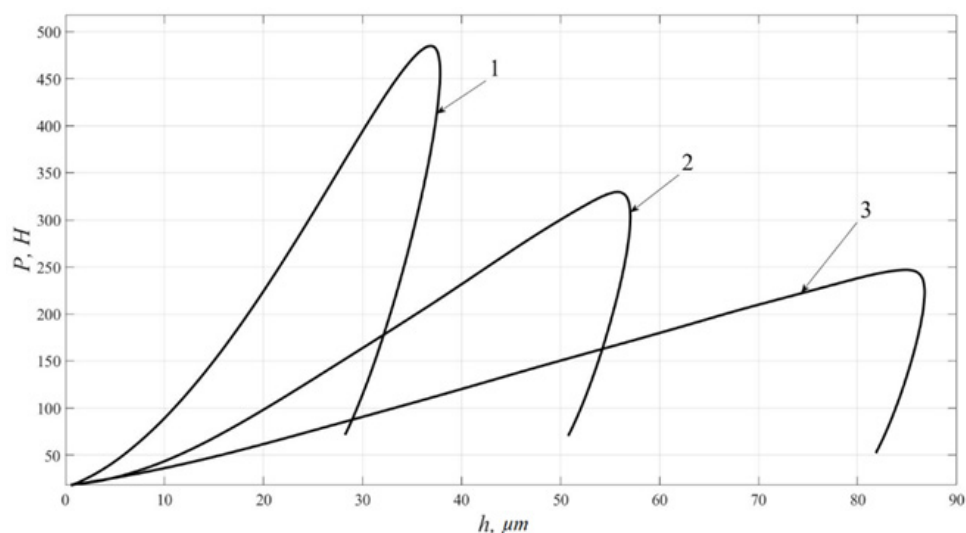
Figure 9. Load–displacement diagram curves for steel (1), brass (2) and aluminum (3) test blocks.

According to the obtained load–displacement curves, the parameters of the indentation, such as the maximal load of indentation, the maximal and residual depth of indentation, and the dissipated and elastic energy of indentation were calculated and are presented in Table 2. In addition, the contact pressure under the indenter was calculated as the ratio of maximal load P_{max} and the contact area S_{res} calculated from the measured residual depth and the known indenter radius.

Table 2. Parameters of indentation.

Test Piece	HV	Maximal Load P_{max}, H	Maximal Depth, μm	Residual Depth, μm	Dissipated Energy, mJ	Elastic Energy, mJ	Contact Pressure P_{max}/S_{res}, MPa
Al	30	247	87	81	10.8	0.7	320
Cu	78	330	57	50	10.1	1.4	689
Fe-C	206	485	38	28	8.7	2.8	1824

4. Discussion

The results achieved in this article prove the possibility of using modified Leeb impact devices with a displaced induction coil for implementation of the dynamic instrumented indentation method.

The obtained results made it possible to construct a load–displacement curve $P(h)$ similar to the well-known instrumented indentation method. This data made it possible to determine the values of the dissipated and elastic impact body energy, the maximal load of indentation, the maximal and residual penetration depth, and the geometric parameters of the indentation region, namely the contact area of the indenter with the surface and the volume of the displaced material. The listed parameters of the indentation process will allow us to measure the contact and volume hardness, the elastic modulus and the yield strength of test objects with portable hardness testers.

Due to the widespread use of Leeb hardness testers and their simplicity of modification, the proposed method of measuring hardness can be quickly implemented. The use of the method of dynamic instrumented indentation will make it possible to carry out testing directly on test pieces of a variety of products, including those used in areas with high responsibility, and to diagnose a wide range of mechanical properties without additional measurements and expensive equipment.

References

1.   Armstrong, R.W.; Elban, W.L.; Walley, S.M. Elastic, plastic, cracking aspects of the hardness of materials. *Int. J. Mod. Phys. B* **2013**, *27*, 1330004. [CrossRef]
2.   Tabor, D. *The Hardness of Metals*; Oxford University Press: Oxford, UK, 2000.
3.   Herrmann, K. (Ed.) *Hardness Testing: Principles and Applications*; ASM International: Russell Township, OH, USA, 2011; p. 255.
4.   Matlin, M.M.; Kazankin, V.A.; Kazankina, E.N.; Kostyukov, V.A. Hardness Control of Large Metal Articles (Survey of Published Studies). *Chem. Pet. Eng.* **2021**, *56*, 835–840. [CrossRef]
5.   Gogolinskii, K.V.; Syasko, V.A.; Umanskii, A.; Nikazov, A.A.; Bobkova, T.I. Mechanical properties measurements with portable hardness testers: Advantages, limitations, prospects. *J. Phys. Conf. Ser.* **2019**, *1384*, 012012. [CrossRef]
6.   *ISO 18265:2013*; Metallic Materials—Conversion of Hardness Values. ISO: Geneva, Switzerland, 2013.
7.   Formisano, A.; Dessì, E., Jr.; Chiumiento, G. Non-Destructive Tests on Carpentry Steels. *Open Constr. Build. Technol. J.* **2019**, *13*, 214–249. [CrossRef]
8.   Liu, D.; Liu, X.; Fu, F.; Wang, W. Nondestructive Post-fire Damage Assessment of Structural Steel Members Using Leeb Harness Method. *Fire Technol.* **2020**, *56*, 1777–1799. [CrossRef]
9.   Leeb, D. Dynamic hardness testing of metallic materials. *NDT Int.* **1979**, *12*, 274–278. [CrossRef]
10. Kompatscher, M. Equotip—Rebound hardness testing after D. Leeb. In Proceedings of the IMEKO TC5 Conference on Hardness Measurements Theory and Application in Laboratories and Industries HARDMEKO 2004, Washington, DC, USA, 11–12 November 2004; pp. 66–72. Available online: https://www.imeko.org/publications/tc5-2004/IMEKO-TC5-2004-014.pdf (accessed on 26 December 2021).
11. Vriend, N.M.; Kren, A.P. Determination of the viscoelastic properties of elastomeric materials by the dynamic indentation method. *Polym. Test.* **2004**, *23*, 369–375. [CrossRef]
12. Anton, R.J.; Subhash, G. Dynamic Vickers indentation of brittle materials. *Wear* **2000**, *239*, 27–35. [CrossRef]
13. Tabor, D. A Simple Theory of Static and Dynamic Hardness. *Proc. R. Soc. Lond. Ser. A-Math. Phys. Sci.* **1948**, *192*, 247–274. [CrossRef]
14. Johnson, K.L. Dynamic effects and impact. In *Contact Mechanics*; Cambridge University Press: Cambridge, UK, 2013. [CrossRef]
15. Subhash, G.; Koeppel, B.; Chandra, A. Dynamic Indentation Hardness and Rate Sensitivity in Metals. *J. Eng. Mater. Technol.* **1999**, *121*, 257–263. [CrossRef]
16. Sundararajan, G. Understanding dynamic indentation behaviour of metallic materials. *Mater. Sci. Technol.* **2012**, *28*, 1101–1107. [CrossRef]
17. Calle, M.A.G.; Mazzariol, L.M.; Alves, M. Strain rate sensitivity assessment of metallic materials by mechanical indentation tests. *Mater. Sci. Eng. A* **2018**, *725*, 274–282. [CrossRef]
18. Almasri, A.H.; Voyiadjis, G.Z. Effect of Strain Rate on the Dynamic Hardness in Metals. *J. Eng. Mater. Technol.* **2007**, *129*, 505–512. [CrossRef]
19. Arizzi, F.; Rizzi, E. Elastoplastic parameter identification by simulation of static and dynamic indentation tests. *Model. Simul. Mater. Sci. Eng.* **2014**, *22*, 35017. [CrossRef]
20. Maki, S.; Yamamoto, T. Computer Simulation of Micro Rebound Hardness Test. *Procedia Eng.* **2014**, *81*, 1396–1401. [CrossRef]
21. Lee, A.; Komvopoulos, K. Dynamic spherical indentation of strain hardening materials with and without strain rate dependent deformation behavior. *Mech. Mater.* **2019**, *133*, 128–137. [CrossRef]
22. Lu, J.; Suresh, S.; Ravichandran, G. Dynamic indentation for determining the strain rate sensitivity of metals. *J. Mech. Phys. Solids* **2003**, *51*, 1923–1938. [CrossRef]

23. Ito, K.; Arai, M. Simple estimation method for strain rate sensitivity based on the difference between the indentation sizes formed by spherical-shaped impactors. *Int. J. Mech. Sci.* **2021**, *189*, 106007. [CrossRef]

24. Xiaoyan, N.; Shenzhen, L.; Xuchen, G.; Cong, C.; Jiang, Z. Design and theoretical analysis of dynamic indentation experimental device. *Mater. Today Commun.* **2020**, *25*, 101275. [CrossRef]

25. Oliver, W.C.; Pharr, G.M. Measurement of hardness and elastic modulus by instrumented indentation: Advances in understanding and refinements to methodology. *J. Mater. Res.* **2004**, *19*, 3–20. [CrossRef]

26. Rudnitsky, V.A.; Djakovicht, V.V. Material testing by the method of dynamic indentation. *Nondestruct. Test. Eval.* **1996**, *12*, 253–261. [CrossRef]

27. Rudnitskii, V.A.; Rabtsevich, A.V. Method of dynamic indentation for evaluating the mechanical characteristics of metallic materials. *Russ. J. Nondestruct. Test.* **1997**, *33*, 266–271.

28. Rudnitsky, V.; Djakovich, V. The Estimation of Elastic Modulus of Metallic Materials by Dynamic Indentation Method. *Mater. Sci. Forum* **1996**, *210–213*, 391–396. [CrossRef]

29. Rudnitsky, V.A.; Kren, A.P.; Lantsman, G.A. Determining Yield Strength of Metals by Microindentation with a Spherical Tip. *Russ. J. Nondestruct. Test.* **2019**, *55*, 162–168. [CrossRef]

30. Kren, A.P.; Rudnitskii, V.A. Determination of the Strain-Hardening Exponent of a Metallic Material by Low-Speed Impact Indentation. *Russ. Met. (Metally)* **2019**, *2019*, 478–483. [CrossRef]

31. *ISO 16859-1-3*; Metallic Materials—Leeb Hardness Test. ISO: Geneva, Switzerland, 2015.

32. Gogolinskii, K.; Syasko, V.; Umanskii, A.; Kazieva, T.; Gubskiy, K.; Kuznetsov, A.; Gluhov, R. Impactor velocity measurement system for dynamic hardness testers and calibration machines on Leeb scales. *Measurement* **2021**, *173*, 108632. [CrossRef]

33. Syasko, V.; Nikazov, A. Research and Development of Metrological Assurance Elements for Leeb Hardness Measurements. *Inventions* **2021**, *6*, 86. [CrossRef]

34. Rudnitsky, V.; Kren, A.; Matsulevich, O. Magnetic Induction Transducer for Dynamic Indentation Hardness Measurements. Republic of Belarus Patent 99117098, MPK G 01N 3/48, 2001.